Mechanism of Ethanol Photo-Oxidation on Anatase TiO_2 (101) Single Crystal

K. Katsiev[1], G. Harrison[2], H. Alghamdi[1], Y. Alsalik[1], A. Wilson[2], G. Thornton*[2], and H. Idriss[1,2]*

[1]Fundamental Catalysis, SABIC-CRD at KAUST, Thuwal, Saudi Arabia

[2]Department of Chemistry and London Centre for Nanotechnology, University College London, London, UK.

*Emails: idrissh@sabic.com and h.idriss@ucl.ac.uk; g.thornton@ucl.ac.uk

Abstract

Despite the proven properties of the anatase phase of TiO_2 related to photocatalysis, detailed mechanistic information regarding a photo-oxidation reaction has not yet been derived from single crystal studies. In this work, we have studied the photo-oxidation of ethanol (as a prototype hole scavenger organic molecule) adsorbed on an anatase TiO_2 (101) surface by STM and on-line mass spectrometry to determine the adsorbate species in the dark and UV illumination in the presence of O_2 and to extract kinetic reaction parameters under photo-excitation. The reaction rate for the photo-oxidation of ethanol to acetaldehyde is found to depend on the O_2 partial pressure and surface coverage, where the order of the reaction with respect to O_2 is close to 0.15. Carbon-carbon bond dissociation leading to CH_3 radicals in the gas phase was found to be a minor pathway, which is contrary to the case of rutile TiO_2 (110) single crystal. Our STM images distinguished two types of surface adsorbates upon ethanol exposure that can be attributed to its molecular and dissociative modes. A mixed adsorption is also supported by our DFT calculations in which we determine similar Energies of adsorption (E_{ads}) for molecular (1.11 eV) and dissociative modes (0.93 eV). Upon UV exposure at (and above) 3×10^{-8} mbar O_2, a third species is identified on the surface as a reaction product, which can be tentatively attributed to acetate/formate species on the basis of C1s XPS results. The kinetics of the initial oxidation steps are evaluated using the STM and mass spectrometry data.

1. Introduction

In spite of the importance of oxide semiconductors in photocatalysis, fundamental studies of well-defined oxide surfaces have not yet received the required attention to construct reliable mechanistic pathways. Among all metal oxides surfaces, TiO_2 is the most understood at the atomic level[1,2,3]. TiO_2 exists in many stable phases, with the most relevant for photocatalysis being the anatase phase[4,5,10,6]. However, most photoreaction studies on well-defined single crystal surfaces have been conducted on the rutile phase[7,8,9], with very little work on anatase. Alcohol chemistry on metal[7,10,11] and oxide[12,13,14,15] surfaces provides a wealth of fundamental information needed to understand catalytic reactions in particular when conducted on model surfaces. Ethanol adsorption and its associated photochemical activity have been studied on powder polycrystalline TiO_2 samples for decades[10,16,17,18,19], although there are no existing experimental studies of ethanol on the TiO_2 anatase (101) surface (the most thermodynamically stable surface). There have been several studies involving other molecules. For instance, methanol adsorption has been studied by TPD[20,21], where molecular adsorption/desorption was evidenced. The photo-oxidation of methanol was studied using 266 nm light at 100 K with TPD and TOF mass spectrometry. Infra-red (IR) spectroscopy was also used to determine the cross-section for the photo-oxidation of CO to CO_2 by one of the present authors in the presence of O_2 at 100 K, and this was found to be substantially greater than for rutile TiO_2 (110)[22]. A recent study of acetaldehyde photoreaction at 100 K demonstrated the cross-coupled formation of 2-butanone[23]. Finally, a recent DFT study of ethanol[24] on TiO_2(101) predicts that molecular adsorption is favored over dissociation.

Reactions of oxygenates on photo-excited TiO_2 are thought to proceed through a hole scavenging mechanism[25]. Upon UV excitation, electrons are transferred from the valence band (VB) to the conduction band (CB) of the semiconductor. In single crystal studies of ethanol photo-oxidation, it has been demonstrated that background O_2 is required. The mechanism inferred involves excited electrons in the conduction band being transferred to O_2 forming $O_2^{\cdot-}$ (oxygen anion radical), which decreases the electron-hole recombination rate[26]. Under UHV conditions, the first step in the photo-oxidation of ethoxides to acetaldehyde on rutile TiO_2 (110) surfaces involves hydrogen atom removal from the α-carbon group. The amount of acetaldehyde detected in the gas phase was found to increase with an increasing dose of O_2. Some of the acetaldehyde undergoes a further oxidation step and is ultimately converted, via carboxylate species, to CO_2[27,28]. The formation of formate/acetate intermediates on the surface was revealed by XPS, where the presence of a –COOH feature in the C 1s spectrum is observed after UV light exposure in the presence of O_2[29]. This is similar to powder results where the photo-oxidation of primary and secondary alcohols as well as ketones leads to the formation of carboxylate species as studied by in situ IR spectroscopy[16,19,30,31,32,33].

In this study, we have investigated the photo-catalytic decomposition of ethanol on an anatase TiO_2 (101) single crystal in order to probe its reactivity and obtain accurate kinetic parameters (photo-reaction cross section, reaction order and rate constants) in a controlled environment. We use STM and mass spectrometry to determine the reaction rates with complementary XPS measurements and DFT calculations.

2. Experimental and Computational Details

The mass spectrometry and STM measurements were performed in a UHV system operating at a base pressure of 1×10^{-10} mbar. The setup is equipped with an Aahrus 15 HT variable temperature STM by SPECS and a HALO 301 residual gas analyzer (RGA) by Hiden Analytical. All STM measurements were carried out at room temperature. The system is also equipped with a sputter gun and separate oxygen, argon, and ethanol gas lines that are fitted with precision UHV leak valves. For TPD measurements, the RGA was mounted inside a Pyrex shroud with a 5 mm aperture to enhance detection from the surface. During the mass spectrometry measurements (with or without UV illumination), the sample was positioned ≤1 mm away from the aperture. A 300 W MAX-303 Asahi Spectra Xe lamp was used as a source of the UV light. The UV light produced by the Xe lamp was delivered to the sample using fiber optics and a focusing lens assembly. An illumination power close to 5 mW/cm^2 was measured for the wavelengths ranging from 310 to 400 nm.

XPS was performed in a separate UHV system with a base pressure of 2×10^{-9} mbar equipped with SPECS XR50 dual anode X-ray source (Mg Kα was utilized) and Scienta R3000 hemispherical electrostatic energy analyzer. Also, the system has a sputter gun and separate oxygen, argon and ethanol gas lines fitted with precision UHV leak valves. A transparent standard UHV port window was positioned for UV illumination.

The anatase TiO_2(101) single crystal (3×3×1 mm^3) was purchased from Pi-Kem, mounted onto a Ta sample plate using Ta foil. The standard procedure for preparing the anatase surface was to perform cycles of Ar^+ sputtering (1×10^{-5} mbar, 1 kV, 20 minutes, 6 μA of drain current) and annealing at 700°C for 15 minutes with the temperature of the sample being monitored using Sirius pyrometer by Process Sensors and a calibrated K-type thermocouple.

The cleanliness of the sample surface was checked using STM. The clean anatase TiO_2 (101) surface displays a stepped sawtooth like surface of unit cell dimensions 10.24×3.78 Å^2 and a step height of 3.8 Å. The unit cell dimensions were used to calibrate the STM in-plane dimensions, while the step height was employed for out-of-plane calibration. In this study, a monolayer (ML) is defined with respect to the number of Ti_{5c}-O_{2c} pairs on an ideal planar anatase TiO_2 (101) surface *i.e.* 5.17 $\times10^{14}$ pairs of atoms per cm^2. A glass vial containing ethanol was connected to the UHV chamber via a high-precision leak valve located 10 cm away from the sample in the dosing configuration. The ethanol (99.85 % purchased from VWR) line was cleaned using standard freeze-pump-thaw cycles. The dose of ethanol exposure is given in Langmuir (L). Oxygen (99.9%) was introduced into the chamber using a high-precision leak valve. The anatase surface was exposed to O_2 for ~3 minutes at the designated pressure prior to opening the UV light shutter. In the photoreactions conducted in the STM chamber, the time frame upon dosing and starting the measurements is two minutes and each run was conducted for two minutes while monitoring the gas phase molecules (m/e 44 (CO_2, CH_3CHO), 31 (CH_2OH^+), 29 (CHO^+), and 15 (CH_3^+)) by the mass spectrometer.

Density Functional Theory (DFT) has been employed using the Quantum Espresso code[34]. Calculations are performed using a generalized gradient approximation (GGA) for ionic cores description along with Perdew-Burke-Ernzerhof (PBE) exchange correlation and GBRV ultrasoft pseudopotentials[35]. All atomic orbitals are considered filled and part of the core potential except for the titanium 3s, 3p, 3d, 4s; oxygen and carbon 2s, 2p; and the hydrogen 1s. For energy minimization, the specified total energy and total forces convergence thresholds are 1×10^{-6} Ry and 1×10^{-4} Ry/Bohr, respectively. The used total kinetic energy cutoffs for wavefunction and density are 50 and 200 Ry, respectively. A (3×3×1) Monkhorst-Pack *k*-point grid is used for all the computations. To obtain smooth results, Gaussian smearing with 0.02 Ry (0.27 eV) spreading for Brillouin zone integration across the Fermi level is used. The employed convergence threshold for self-consistency is 1×10^{-6}. A 2×2 five layer slab of anatase TiO_2 (101) has been built from optimized parameters of the bulk TiO_2 anatase unit cell. The optimized unit cell parameters are a = 3.802

Å, c = 9.697 Å, and u = 0.2066, yielding a cohesive energy of 24.5 eV at a volume of 35.1 Å^3. The computed bulk modulus (B_0) is 185.2 GPa and its derivative (B_0') is 4.47 GPa; calculated using the Murnaghan equation of state[36]. The vacuum distance on top of the slab is set to 15 Å. In this study, the bottom layer is fixed to simulate bulk properties, and the top four layers were allowed to relax. Isolated gas-phase molecules were simulated in 15×15×15 Å periodic cell. The adsorption energy (E_{ads}) is defined by the equation shown below.

$$E_{ads} = E_{ads+TiO2} - [E_{bareTiO2} + E_{EtOH}]$$

Where $E_{ads+TiO_2}$ is the energy of the adsorbed molecule on TiO_2, E_{EtOH} is the energy of isolated ethanol molecule and $E_{bareTiO2}$ is the energy of the clean surface. In this study, the adsorbate coverage is set to 25%. Dispersion interaction forces have been included through the use of the DFT-D2 method by Grimme to study the effects of weak interactions such as London forces in the adsorbate-semiconductor system[37].

3. Results and discussion

3.1 Scanning Tunneling Microscopy (STM) of CH_3CH_2OH - TiO_2(101) anatase single crystal

The surface morphology of a clean freshly prepared anatase (101) crystal, studied by STM, showed wide terraces of 30 nm in size (**Figure 1A**) with straight step edges oriented along the [010], [$\bar{1}$11], and [11$\bar{1}$] principal directions forming triangular terraces from which the [10$\bar{1}$] orientation can be identified (i.e. directed towards the base[38]). The atomically resolved STM image of the pristine surface shown (**Figure 1B**) allows the identification of the "non-primitive centered" surface unit cell of 10.24×3.78 Å^2 (indicated by black rectangle) and 1×1 periodicity. The bright round features observed at the surface are attributed to contaminants. These are at ca. 1% of surface coverage and attributed to adventitious carbon, and consistent with C 1s XPS data that also indicated the presence of carbon in trace amounts. The dark features indicated by a blue rectangle are associated with more reduced TiO_{2-x} anatase surfaces; sub-surface oxygen-vacancies that resulted from vacuum annealing[26,39] (as demonstrated in previous STM studies performed on anatase TiO_2 (101) single crystal surfaces).

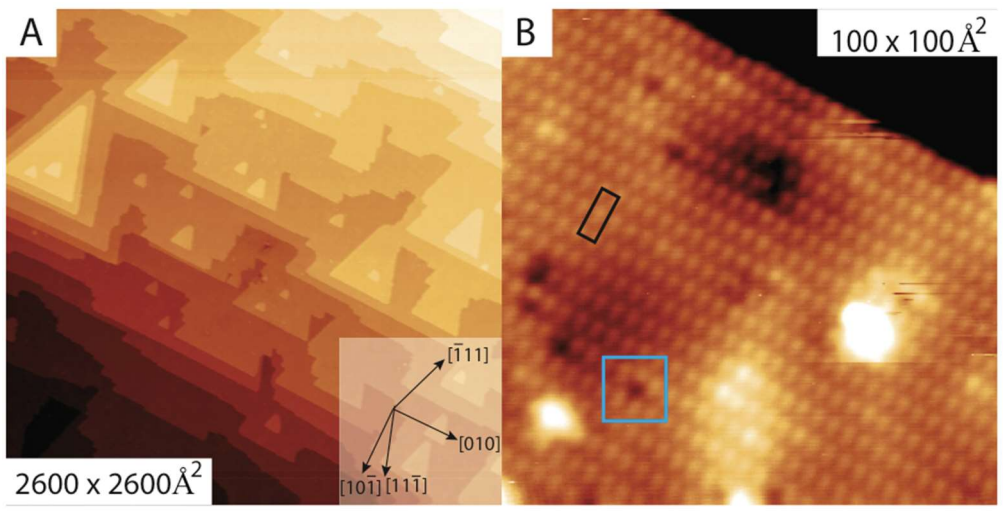

Figure 1.
STM of a clean TiO_2 anatase single crystal. **(A)** A large scale image of a clean and prepared anatase TiO_2 (101) (at 2700×2700 Å^2 resolution, 1.65 V, and 0.15 nA). **(B)** A high resolution image (at 100×100 Å^2, 1.65 V, and 0.2 nA). The blue box identifies a depression centred on Ti_{5c}-O_{2c} in the empty state image, most likely due to a sub-surface O_{vac}. The black box identifies the surface unit cell, 10.24×3.78 Å^2.

The surface shown in **Figure 1** was exposed to 18 L of ethanol at 300 K (**Figure 2A**). Round bright features representing a coverage of 8.5% ML of ethanol were observed on the surface as both clusters and isolated features. A mean sticking coefficient, S, of 0.03 was determined for an ethanol exposure of 3 L and this value decreased to 0.007 after a 50 L exposure indicating a relatively weak surface-adsorbate interaction. For comparison, using similar dosing conditions, Grinter *et al*.[40] determined a mean sticking coefficient of ~1 for a low coverage (0.1 L, 1 Langmuir = 1.33 x 10^{-6} mbar s) of acetic acid adsorbed at room temperature. The difference between the sticking coefficients of acetic acid and ethanol is related to the strong adsorption energy of the former when compared to the latter.

Two distinct tunneling modes were observed, with ethanol appearing as bright features of ~6 Å diameter spread over the Ti_{5c}–O_{2c} positions (**Figure**

2A) or as bright-dark-bright features spanning three Ti_{5c}–O_2c pairs (see **Figure 2A** inset where a defect is circled as well as zoom of inset). These were found to be equivalent in location by monitoring STM contrast changes. This behavior has been reported on anatase (101) for water where it is attributed to the change in the metallic character of the tip, where coordination of H_2O results in a redistribution and change in energy of the LDOS at the Ti-O stite, and observed as a depression in the empty state image.[41,42] A higher density of ethanol molecules is observed at the bottom of step edges as opposed to upper step edge, as a result of ethanol diffusion at RT. This is in contrast to the stronger binding of acetic acid, which shows no preference for terrace or step edges[40]. Scanning Tunneling Spectroscopy (STS) measurements by Diebold and co-workers indicated that excess electrons can be trapped at the upper and lower step edges leading to a preference there for O_2 adsorption[43].

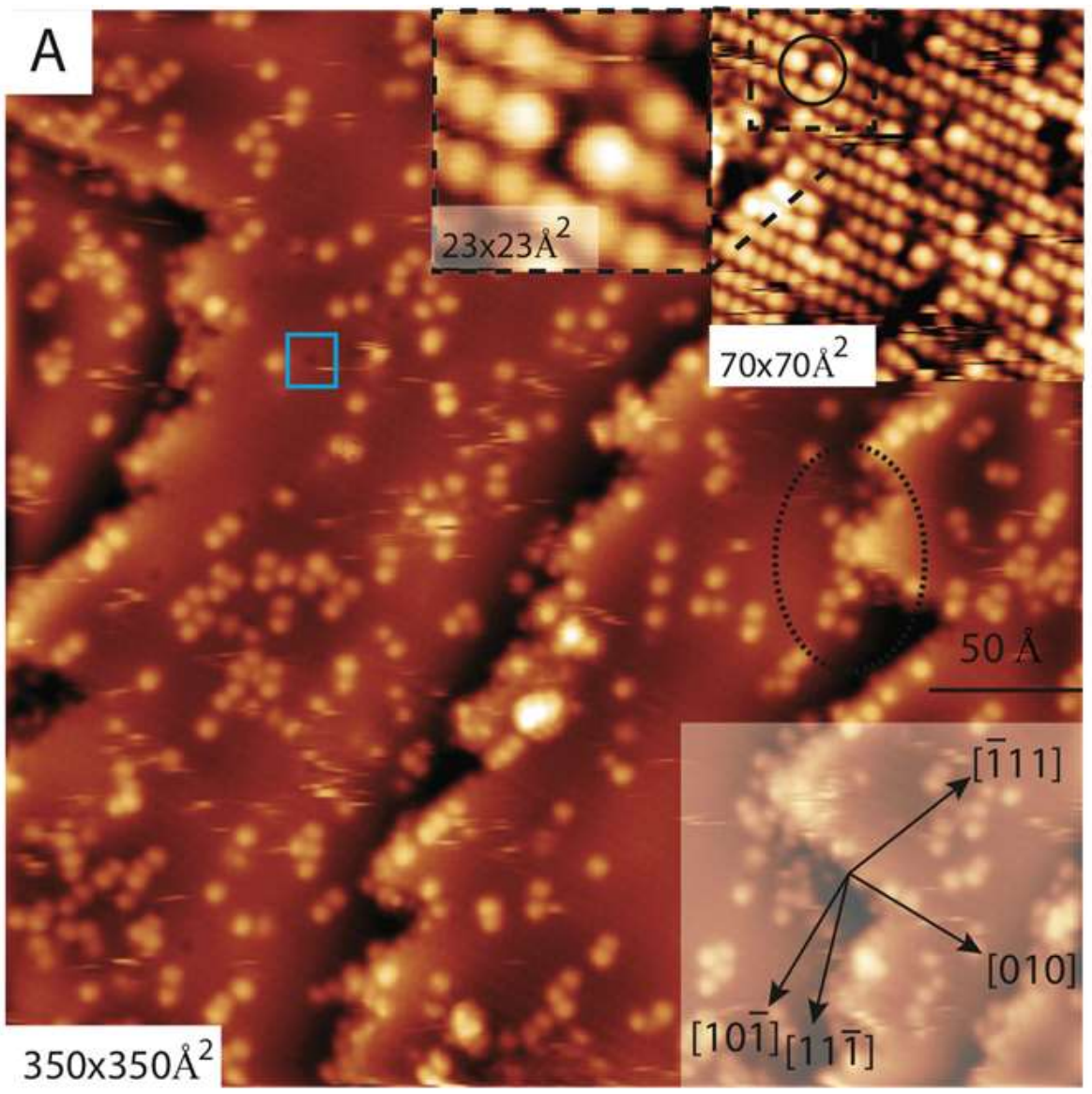

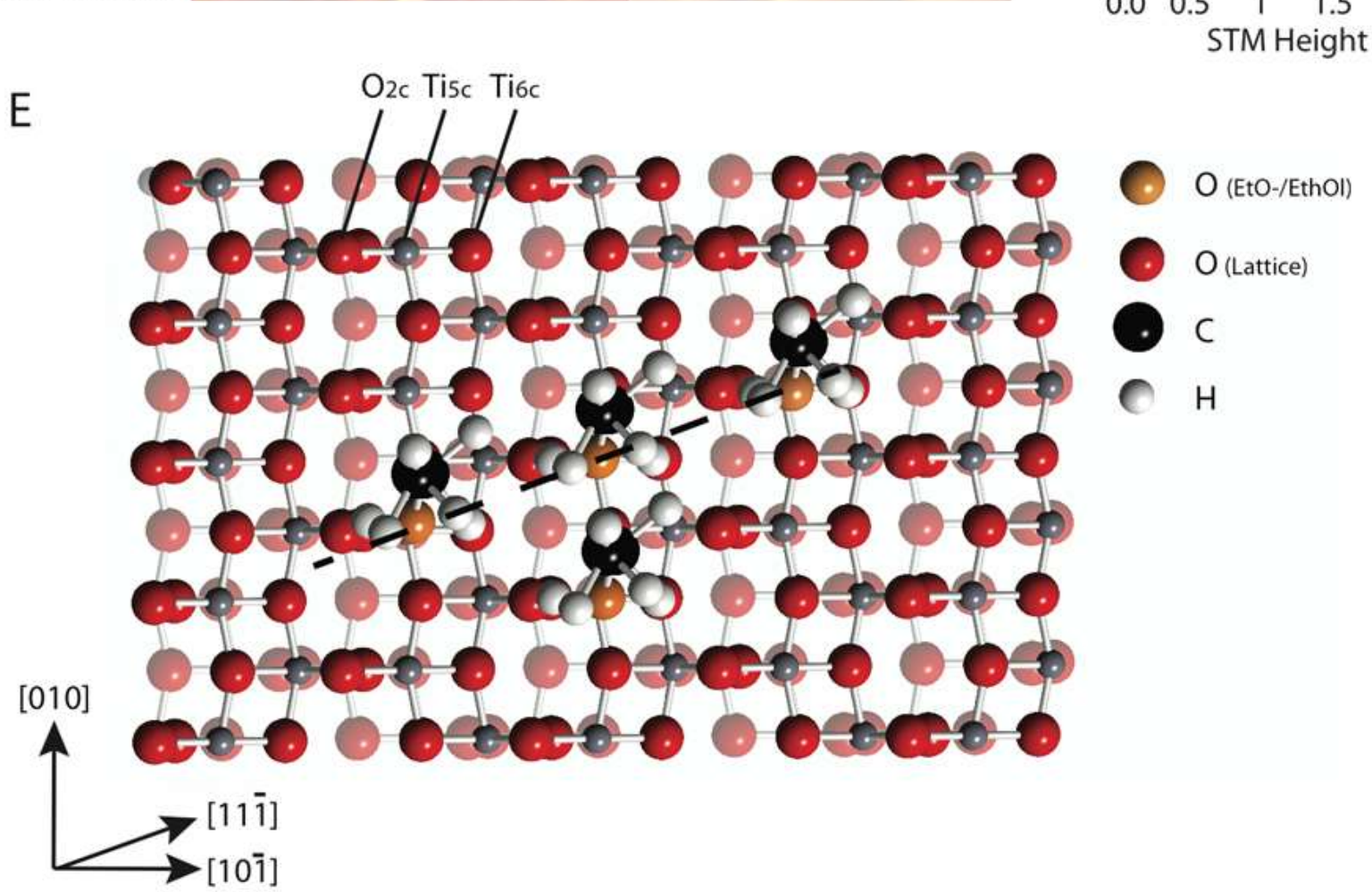

Figure 2.
STM images of anatase TiO_2 (101) after exposure to 18 L of ethanol at 300 K. **(A)** 350×350 $Å^2$ resolution, 2 V, 0.420 nA, with 0.085 ML EtOH/EtO– coverage. The blue square represents a feature associated with O_{vac}. The black oval shows an example of ethanol clustering at the step edges. Upper inset: (70×70 $Å^2$) ethanol on anatase TiO_2 (101) in 'depression' contrast where the black circle indicates EtOH/EtO–; a zoom of this feature is shown. Lower inset: the principal azimuths of anatase TiO_2 (101). **(B)** A zoom of (A); a (70×70 Å) image where the blue and green circles represent 1.7 Å and 1.2 Å protrusions, respectively. Blue line: line of the STM profile shown in (C). White dashed lines: arrangements of protrusions in the $[\bar{1}11]$ and $[11\bar{1}]$ directions. **(C)** Line profile from (B) where ~1.2 Å and ~1.8 Å (1.7 in fig) height species can be identified**. (D)** Histogram of the measured heights of 495 particles from the 350×350 Å image in (A**)** with a bin width of 0.1 Å. (**E**) A model of the (101) surface with EtOH/EtO- molecules coordinated to the Ti_{5c}.

Short chains of the adsorbed ethanol molecules with separation of ~5.5 Å are observed with preferential orientations along the $[1\bar{1}1]$ and $[11\bar{1}]$ directions. This suggests co-ordination of ethanol in adjacent sites along the [010] direction, with the C–C moiety oriented perpendicular to the titanium rows. Similar arrangements of acetic acid and water on anatase TiO_2 (101) have been demonstrated by STM[44,40]. A simple steric requirement can explain the arrangement: the short side of the surface unit cell is ~3.7 Å would prevent adsorption on two neighboring Ti cations. This is shown in the covalent radii ball and stick model of the (101) surface in Fig. 2E, where ethanol molecules are coordinated to Ti_{5c} , forming a chain in the $[11\bar{1}]$ direction. In the model two molecules are shown positioned on nearest Ti_{5c} neighbors.

Ethanol imaged at positive sample bias on the surface at 300 K revealed two apparent heights as shown in **Figures 2C,D**. These can be attributed to the two adsorption modes: molecular and dissociated. A previous DFT study of ethanol adsorbed on anatase TiO_2 (101) indicated a preference for molecular adsorption with co-ordination of the ethanol to the Ti_{5c}[24]. The different heights could also be due to ethanol and water being co-adsorbed together, but this is discounted by the lack of a water signal in the mass spectrometry data (although there is no guarantee that the water would be desorbed by UV). The STM heights of the adsorbates in the image of **Figure 2A** were measured (total area of 135,000 $Å^2$). The histogram in **Figure 2D** with a bin width of 0.1 Å allows the determination of a major peak of 1.8 Å (92%), and two minor ones of 1.2 Å (5%) and 2.4 Å (3%). Hansen *et al.*[45] reported a difference in STM height of 0.5 Å between two species attributed to EtOH (2.6 Å) and EtO– (2.0 Å) bound to Ti_{5c} on rutile TiO_2 (110). On this basis the majority species on anatase TiO_2 (101) is assigned to EtO- (1.7 Å), with EtOH at 2.4 Å (the minor contribution to the 1.2 Å could not be assigned). A DFT study by Zhang et al.[24] indicated a similar adsorption energy for molecular and dissociative adsorption of ethanol to Ti_{5c} on the perfect surface, with an activation barrier of 0.95 eV. In addition, the dark features that are associated with sub-surface oxygen vacancies are apparently unreactive with ethanol (**Figure 1A**, blue box).

3.2 Density Functional Theory of ethanol and acetaldehyde on TiO_2(101) anatase surface.

DFT calculations were performed to provide a theoretical understanding of ethanol adsorbed on anatase (101). A coverage of 0.25 ML was used, which is close to the upper saturation coverage observed in STM. A similar methodology to Zhang *et al.*[24] has been employed, using a GGA and PBE approach. In addition, we have modeled weak interactions such as London dispersion forces using the DFT-D2 method by Grimme *et al*.[37] We have limited our calculations to co-ordination of ethanol to the Ti_{5c} site, and scission of the O-H bond in ethanol. **Figure 3** depicts ball and stick models of the anatase TiO_2 (101) surface with the relaxed atomic positions, of the adsorbed ethanol and acetaldehyde (as a reaction product that is discussed in the following sections). The atomic positions of the clean perfect surface were obtained, and they compare favorably to previous theoretical DFT work[46,47]. DFT results indicate that the adsorption energies (E_{ads}) are very close for dissociated and molecular adsorption; 1.11 eV for molecular ethanol on the Ti_{5c} (**Figure 3A**) and 0.93 eV for dissociated ethanol on the Ti_{5c} (**Figure 3B**). Additionally, acetaldehyde with identical coordination to that of molecular ethanol (**Figure 3C**) is found to be less stable, with an adsorption energy of 0.77 eV. The inclusion of the dispersion interaction between the adsorbates and TiO_2 lattice lead to greater instability (~0.2 eV) of the dissociated form of ethanol when compared to the molecular one. **Table 1** presents some selected geometry parameters of the ethanol, ethoxide, and acetaldehyde adsorptions.

Among the computed modes, only the dissociated mode of ethanol induces major changes to the TiO_2 surface structure by upward displacement of the Ti_{5c} (0.42 Å), which in turn increases the Ti_{5c}–O_{3c} by 0.38 Å. Acetaldehyde does not show any structural differences when compared to the molecular ethanol other than the 0.23 Å shorter O_{ads}–C1 bond.

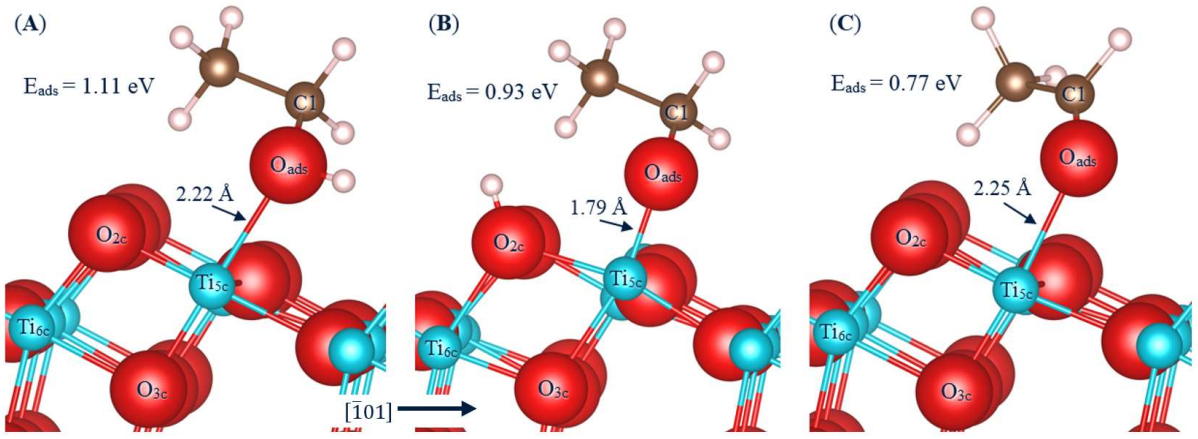

Figure 3.
DFT GGA PBE + D computed parameters for the adsorption of ethanol on a relaxed anatase TiO_2 (101) surface. **(A)** Molecular adsorption of ethanol on Ti_{5c}, E_{ads} = 1.11 eV **(B)** Dissociative adsorption of ethanol on Ti_{5c} and coordination of H to the adjacent O_{2c}, E_{ads} = 0.93 eV. **(C)** Molecular adsorption of acetaldehyde on Ti_{5c}, E_{ads}=0.77 eV. Color designations are as follows, red: oxygen, cyan: titanium, brown: carbon, and white: hydrogen.

Table 1.
Adsorption energies of the bare slab, as well as molecular and dissociated ethanol and acetaldehyde on anatase TiO_2 (101) along with selected geometry parameters (all distances in Å). Atomic labels are shown in **Figure 3.**

Parameter	Bare slab	EtOH-(a)	EtO-(a)	MeCHO-(a)
Adsorption energy, eV	--	**1.11**	**0.93**	**0.77**
O_{ads} – Ti_{5c}	--	2.22	1.79	2.25
O_{ads} – C1	--	1.46	1.42	1.23
Ti_{5c} displacement in *z*-dir. w.r.t. relaxed slab	+0.08*	+0.18	+0.42	+0.13
O_{plane} to C_{plane} (i.e. Ti_{5c} – C1)	--	3.28	3.02	3.21
Ti_{5c} – O_{3c}	1.78	1.87	2.16	1.84
Ti_{6c} – O_{2c}	1.85	1.86	2.04	1.85
O_{2c} – H_{ads}	--	--	0.98	--
• **Ti displacement here is with respect to unrelaxed slab. Ti_{5c} during relaxation moves downward with respect to surface plane, yet, the top three layers slightly reconstruct during geometry optimization by moving upward in the z-direction making the absolute movement of Ti_{5c} positive (i.e. upward).**				

3.3 STM of ethanol photoreaction on TiO_2(101) anatase single crystal

The effect of UV light exposure at 300 K on a 50 L ethanol dosed anatase TiO_2 (101) surface was studied by STM, the results are shown in **Figure 4**. Exposure to UV light in the absence of O_2 showed negligible photoreaction products in the gas phase: H_2, CH_3CHO, CH_3 (radical), in line with previous similar studies on rutile TiO_2 (110)[29,48] and other studies of the reaction of organic molecules on TiO_2 (110) and (011) single crystal surfaces[28,49]. The photo-catalytic reactions after UV exposure in presence of molecular oxygen on the ethanol covered surface at different partial pressures were studied. In each experiment a freshly prepared surface had an identical exposure to ethanol prior to photo-catalysis. For example, at an O_2 pressure of 3×10^{-8} mbar, a depletion of a fraction of the surface could be determined from the coverage of ethanol before and after UV irradiation. A reduction in surface coverage from 0.12 ML to 0.08 ML was observed after 13 minutes at an irradiation of approximately 5 $mWcm^{-2}$. Considering that the Ti_{5c} density is 5.2×10^{14} cm^{-2} for anatase TiO_2 (101), a 0.04 ML decay (depletion rate) in 780 seconds gives a surface depletion of ethanol/ethoxide of 2.67×10^{10} species $s^{-1}cm^{-2}$. The 5 $mWcm^{-2}$ irradiation in the range of 320–390 nm corresponds to approximately 9.2×10^{15} photons $s^{-1}cm^{-2}$ which translates into a reaction rate of about 4×10^{-6} (molecules removed per photon) at an oxygen pressure of 3×10^{-8} mbar.

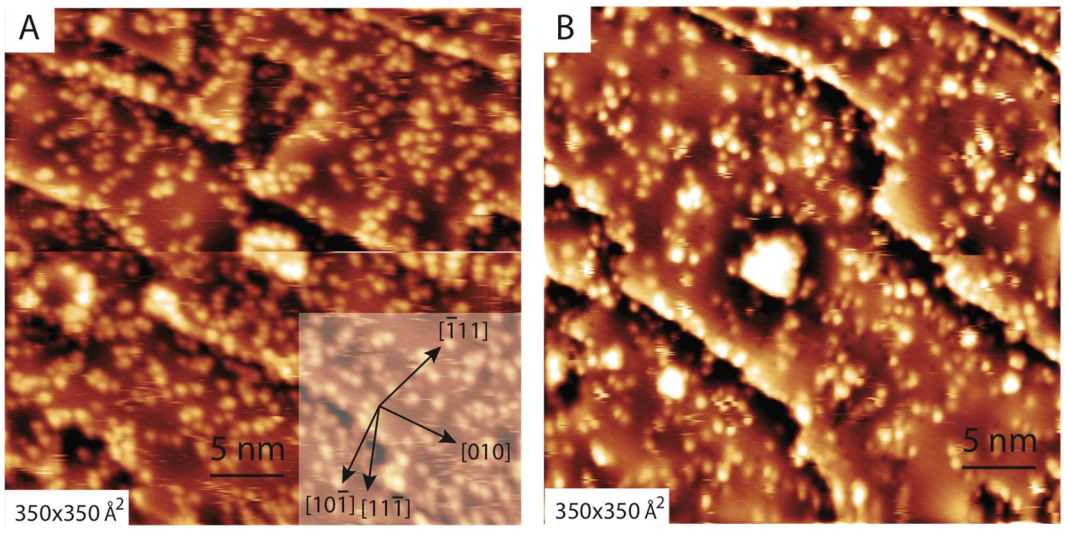

Figure 4.
Representative STM images (350×350 Å^2) of anatase TiO_2 (101) after exposure to 50 L ethanol at 300 K. (**A**) Before UV illumination (2.1 V, 0.64 nA) with an ethanol coverage of 0.12 ML. (**B**) After UV illumination in 3 x 10^{-8} mbar O_2, (2.1 V, 0.29 nA) with an ethanol coverage of 0.08 ML (13 minutes of irradiation at 5 mWcm^{-2} (360 nm)).

3.4 Photo-reaction cross section measurements by STM. Comparison with other compounds and surfaces.

Previous work by others has shown in similar kinetics. For example, White and Henderson found that photolysis of trimethylacetic acid (TMMA) on rutile TiO_2 (110) gave a yield of 1.5×10^{-5} (molecules depleted per photon) for the first 10 s of the reaction based on mass spectrometric data[50]. It is important to note that this type of evaluation is based on results from a single crystal, which has the smallest possible surface to bulk ratio; i.e. one layer of adsorbate in the unit area exposed to light. In real catalytic conditions, particles of nanometer size stacked on top of each are expected to react with the same number of photons. In other words, assuming a homogenous particle size distribution of 10 nm for TiO_2 and a compact stacking perpendicular to the incident light, 100 layers or particles per 1 μm depth (above this distance light will be strongly attenuated) would expose over 200 times the area (**Figure 4**).

A decay mechanism, $C_{(t)}=C_o \exp(-kt)$, for the reaction can be proposed, where $C_{(t)}$ is the number of ethanol molecules on the surface at time t and C_o that at t = 0. The rate constant, k in s^{-1} of the decay, can be extracted from STM data: $\mathrm{Ln}(C_o/C_{(t)})/t = k$ or $\mathrm{Ln}(0.12/0.08)/780\mathrm{s} = 0.0012\ \mathrm{s}^{-1}$. Since $k = F\times A$ where F is the photon flux and A the cross sectional area, a photon flux F of 9.2×10^{15} photons s^{-1}cm^{-2} gives a cross-section of 1.2×10^{-19} cm^2. Cross-sectional areas for other reactions on TiO_2 rutile single crystal were calculated before by us and others using on line mass spectrometers, RAIRS, or XPS C 1s signals. **Table 2** shows some of the numbers extracted in similar sets of experiments for comparison.

Table 2.
Photooxidation of various oxygenates over the surfaces of oxide single crystals at the given O_2 pressures (P_{O_2}). The cross section A is defined as k/F where k is the rate constant in s^{-1} and F is the light flux in (number of photons)/(cm^2.s)

Molecule	Surface	Cross section (cm^2)	P_{O2} (torr)	Comments
O_2	TiO_2 (110) - rutile	1.5×10^{-15} - 8×10^{-17}	PSD	Reference 51
CO	TiO_2 (110) - rutile	3×10^{-18}	5×10^{-6}	Reference 52
Ethanol	TiO_2 (110) - rutile	2×10^{-18}	1×10^{-6}	Reference **Error! Bookmark not defined.**
Acetaldehyde	TiO_2 (011) - rutile	10^{-17} - 10^{-19}	Pre-dosed	Reference **Error! Bookmark not defined.**
Glycine	ZnO (000$\bar{1}$) - O	$1.5\text{-}2.5\times10^{-18}$	5×10^{-6}	Reference 53
TMAA	TiO_2 (110) - rutile	ca. 10^{-18}	-	Reference 5
Acetic acid	TiO_2 (011) - rutile	9×10^{-22}	1×10^{-6}	Reference 49
Acetone	TiO_2 (011) - rutile	10^{-18} - 3×10^{-21}	5×10^{-7}	Reference 54
Ethanol	TiO_2 (101) - anatase	1×10^{-19}	4×10^{-8}	This work

PSD: Photo-stimulated desorption; TMAA: tri-methyl-acetic acid.

In another experiment, shown in (**Figure 5A,B**), the STM image of an ethanol dosed surface after UV exposure at ~7 mW/cm^2 for 3600 s in the presence of 3×10^{-8} mbar oxygen indicated the existence of large protrusions in the 'depression' mode in addition to ethanol/ethoxides. Such protrusions were not observed prior to UV exposure. These features of 0.01-0.02 ML are arranged in a (1×2) formation along the [010] direction,

where a row of three are displayed in **Figure 5B** (the zoom of **Figure 5A**) with the line profiles in **Figure 5C** indicating a seperation of 10 Å. This is potentially attributed to bidentate binding species, such as acetate.[40]

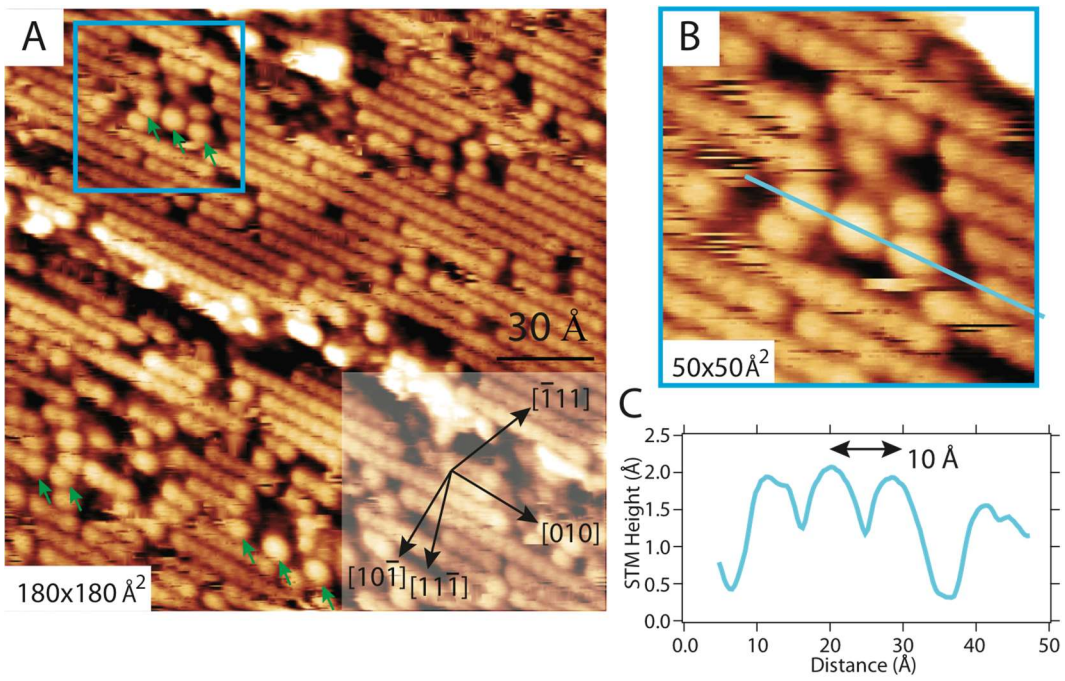

Figure 5.
(**A**) Filtered and polynomial flattened STM image (180×180 Å^2, 2.1 V, 0.25 nA) of anatase TiO_2 (101) after exposure to 50 L ethanol at 300 K and UV illumination in 3 x 10^{-8} mbar O_2. Green arrows outside the cyan box indicate small fractions of different spacing. (**B**) (50×50 Å^2) a zoom of image **A** identified by the cyan box, which contains features in a (1x2) arrangement. (**C**) A height-profile of the line shown in **(B).**

3.5 XPS C1s of ethanol on TiO_2(101) anatase before and after photoreaciton.

To further study the origin of this species, we utilized XPS. The cleanliness of the freshly prepared anatase TiO_2 surface was checked and did not show any significant contaminants. A saturation coverage of ethanol was dosed onto the surface and followed by UV exposure under 1 x 10^{-5} mbar O_2. In order to monitor the reaction products on the surface, C 1s core level spectra were collected before and after the excitation with UV light. The spectrum of the clean surface contained a contribution from tantalum carbide at 282 eV that could not be removed by many sputtering cycles and that was subtracted from both spectra, before and after the UV excitation, and is presented in **Figure 6**. The XPS spectrum before the reaction (**Figure 6A**) has the signature of ethoxides as evidenced by the spectral features at 286.5 and 285 eV due to –CH_2O(a) and –CH_3 groups, respectively. The spectral features and ratios are in accord with XPS data reported for rutile TiO_2 (110)[29]. After UV exposure for 360 s, one can notice a decrease of the C 1s peaks attributed to ethoxides (**Figure 6B**) and the appearance of a peak at 289.5 eV representing about 10% of the total carbon species left on the surface. The latter is attributed to RCOO(a) species[49,55]. However, the decrease of the ethoxides is not mirrored by the increase of carboxylates. In other words, a large fraction of adsorbed ethanol/ethoxides is removed from the surface while a small fraction is oxidized to carboxylates. This is inline with the reaction of adsorbed ethanol under UV excitation studied by on-line mass spectrometry, which is presented below.

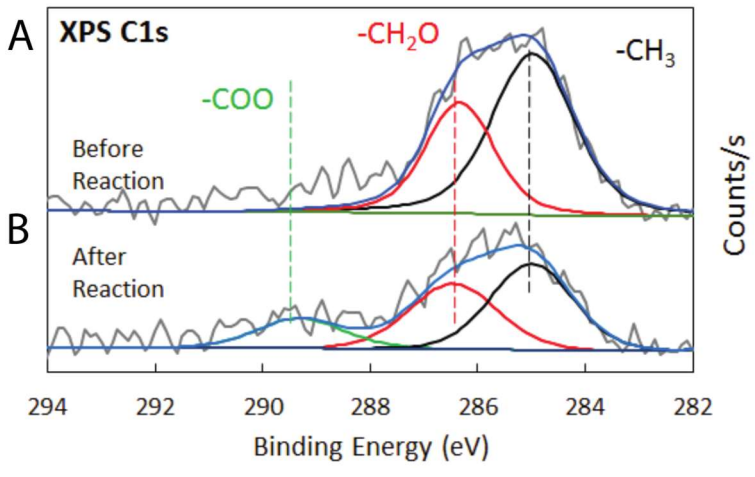

Figure 6.
XPS spectra of anatase TiO_2 (101) surface after a saturation exposure (ca. 100 L) to ethanol before (**A**) and after (**B**) exposure to UV light (light flux: 10^{17} photons $cm^{-2}s^{-1}$ in the 360-400 nm range) at 1×10^{5} mbar O_2. $-CH_2O$ 286.5 eV (red), $-CH_3$ 285 eV (black), $-COO$ 289.5 eV (green).

In order to study the initial reaction parameters, reaction rate, and reaction products, two sets of experiments were conducted. The first involved a saturation exposure of the anatase TiO_2(101) single crystal surface to ethanol at 300 K, followed by UV exposure at ~5 mW/cm^2 in the presence of molecular oxygen at different partial pressures. In the second experiment an O_2 partial pressure of 1×10^{-7} mbar was maintained while changing the surface coverage of ethanol. For each experimental run, the surface was cleaned by repeated Ar^+ sputtering and annealing to 1000 K, then surface cleanliness was checked with STM prior to each run.

Three sets of control experiments were conducted in order to rule out any contribution to the mass spectrometer signal from the background. The desorption products of ethanol were collected (by monitoring m/e 44, 31, 29, and 15) from the back of the Ta sample holder pre-dosed with saturating coverage of ethanol (1), from the surface of the clean anatase TiO_2 (101) crystal at 1×10^{-7} mbar of O_2 (2), and from the anatase surface in UHV, pre-dosed with ethanol (3). In all three cases, desorption products were negligible in quantity when compared to the signal detected from anatase TiO_2 (101) under surface reaction conditions. The main reaction products seen at 300 K are acetaldehyde and CO_2. This is based on their fragmentation patterns of (m/e 44, 31, 29, and 15) and (m/e 44) respectively, and thus were monitored exclusively. Previous results on rutile TiO_2(110) related to photo-oxidation of acetaldehyde indicated the formation of CH_3 radicals[1]. We have checked this route on the anatase surface of this work and found negligible contribution. In a parallel work we have conducted the same set of experiments on rutile TiO_2(110) and indeed found the desorption of CH_3 radicals that was sensitive to oxygen partial pressure.[56] The CH_3 radical (m/e 15) was determined after removal of the contribution from acetaldehyde (~39 %).

The desorption of photochemically produced acetaldehyde in the gas phase is seen to correlate strongly with the presence of oxygen in the UHV chamber and initial coverage (θ) of ethnaol on the surface. Because aldehydes are more weakly adsorbed than alcohols on metal oxides in general and TiO_2 in particular[23,28] (see **Table 1**; $E_{ads,\ acetaldehyde} = 0.77$ *vs.* $E_{ads,\ EtOH} = 1.11$ eV), the former will desorb to the gas phase as soon as they are formed from an ethanol covered surface. **Figure 7A** shows production of acetaldehyde (m/e 29) (deducting 10% of (m/e 31) intensity arising from ethanol) on the (101) surface of anatase TiO_2 as a function of O_2 partial pressure (mbar). After the UV shutter was opened (UV on), a sharp rise in response of mass m/e 29 was observed; this signal then decayed towards a background elevated from the baseline. After closing the UV shutter (UV off), the response decays to a baseline that is determined by the background O_2 pressure and chamber pumping speed. The computation of peak area was made by fitting a linear background in line with the pressure before and after UV light exposure, then integrating the total area as defined by the brown shaded region in **Figure 7B**. A double exponential fitting was found to best represent the desorption trend of acetaldehyde from the surface.

3.6 Effect of O_2 pressure on the photo-oxidation of ethanol on TiO_2(101) anatase single crystal.

The plot of total integrated area against O_2 pressure (**Figure 7C**) displays a logarithmic function, indicating a limiting influence of gas phase O_2 on the reaction rate at ~1×10^{-7} mbar, at which point the adsorption sites on the anatase TiO_2 (101) surface would be saturated. Similar results for ethanol photo-reaction using XPS on the rutile TiO_2 (110) surface were reported. The finite non-zero intercept at 0 O_2 pressure is either suggestive of a small production of acetaldehyde in the absence of O_2 or simply to the uncertainty of the fit. Shown in the inset of **Figure 7C** are the areas of the fast and slow decay processes (associated with the double exponential fitting). The total area for the fast process remains constant as a large fraction of ethanol is depleted within the first 100 second or more. The slow processes contribution however increases with O_2 pressure.

The total rate of depletion, rate = $k\,[P_{O_2}]^{a}\,[\theta_{EtOH}]$, where k is the average of fast k_1 and slow k_2 processes was analyzed by plotting the Ln(peak area) against the Ln(P_{O_2}) at a constant θ_{EtOH} (**Figure 7D**). The reaction order of this photocatalytic reaction with respect to O_2 partial pressure was found to be equal to 0.15.

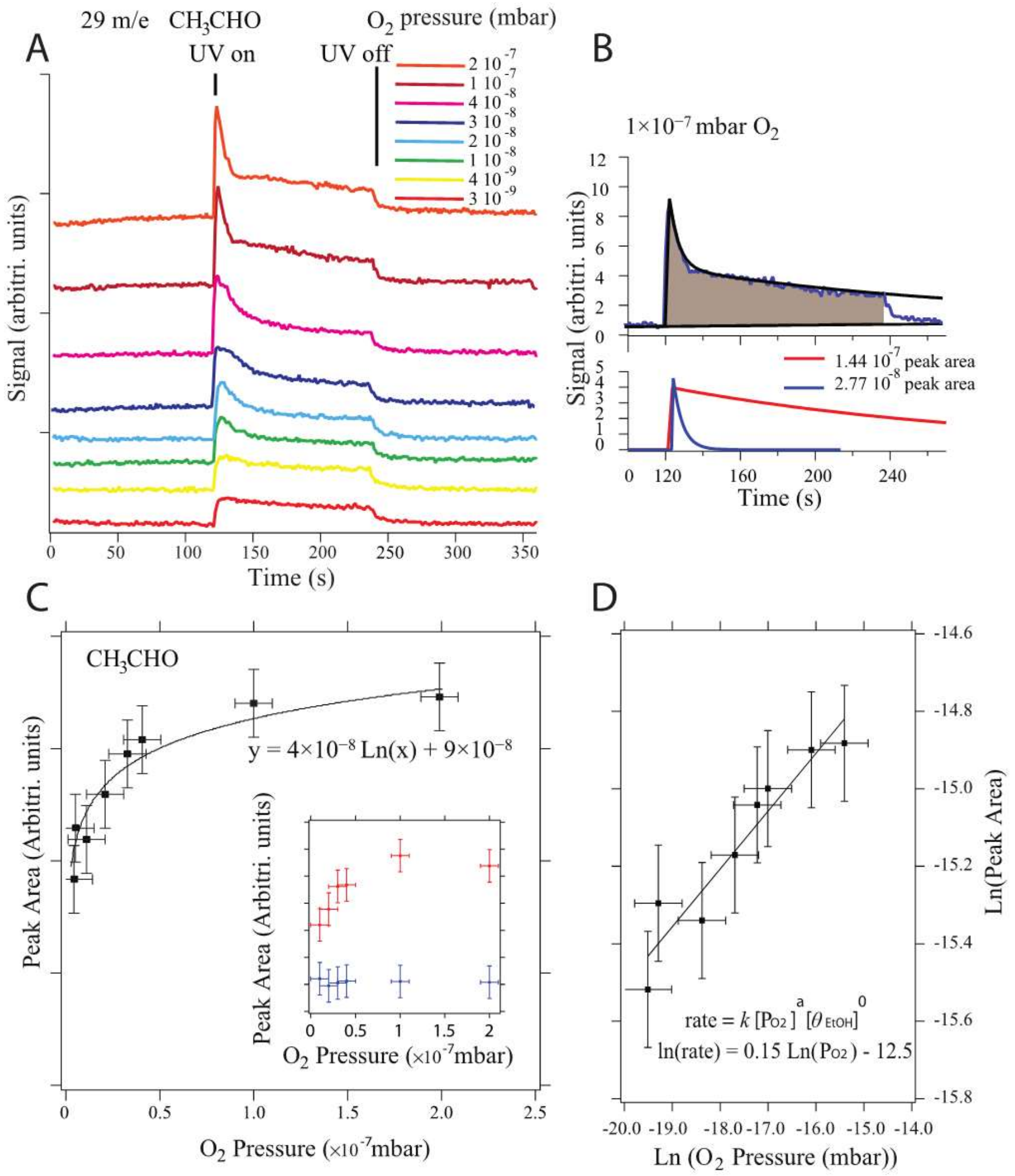

Figure 7.

(**A**) Acetaldehyde formation upon photo-oxidation of ethanol on TiO_2 (101) anatase single crystal at a saturation coverage of ethanol at 300 K, and the indicated molecular O_2 pressures in mbar. UV excitation flux = ca. 5mW/cm^2. (**B**) An example of an exponential fit for the 1×10^{-7} mbar O_2 run, with fast and slow exponential decays, brown shaded region was used. (**C**) Computed peak areas from Figure 7(A) as a function of O_2 pressure in mbar. (**D**) Ln (reaction rate) taken from (A) as a function of Ln(P_{O_2}).

3.7 Effect of ethanol surface coverage on the photo-oxidation of ethanol on TiO_2(101) anatase single crystal.

Figure 8A shows the production of acetaldehyde on anatase TiO_2 (101) where in this case the ethanol exposure was varied in the range of 2.3-23 L at a constant O_2 pressure of 1×10^{-7} mbar. Knowing the chamber volume (3.6 L), the number of acetaldehyde molecules desorbed was obtained, and converted into a fractional coverage desorption rate: $MLs^{-1}cm^{-2}$ of ethanol, where 1 $MLs^{-1}cm^{-2} = 5.2\times10^{14}$ molecules s^{-1}. **Figure 8C** shows a graph of the (initial) rate, r ($MLs^{-1}cm^{-2}$) plotted against initial ethanol coverage, θ_{EtOH}, on the surface. The rate can be expressed as:

$$r = k\,\theta_{EtOH}{}^{a}\,[P_{O_2}]^{0.15}$$

or

$$Ln(r) = Ln(k) + a\,Ln(\theta_{EtOH}) + 0.15\,Ln(P_{O_2})$$

Figure 8D is a Ln(r) against Ln(θ_{EtOH}) plot, giving a reaction order, a, of 1. The rate constant for the reaction could then be extracted and was found to equal 0.049 s^{-1} giving a cross section of 4.7×10^{-19} cm^2, which is in line with the value we obtained (1×10^{-19} cm^2) from the change in surface coverage from STM at $P_{O2} = 4 \times 10^{-8}$ mbar (**table 2**).

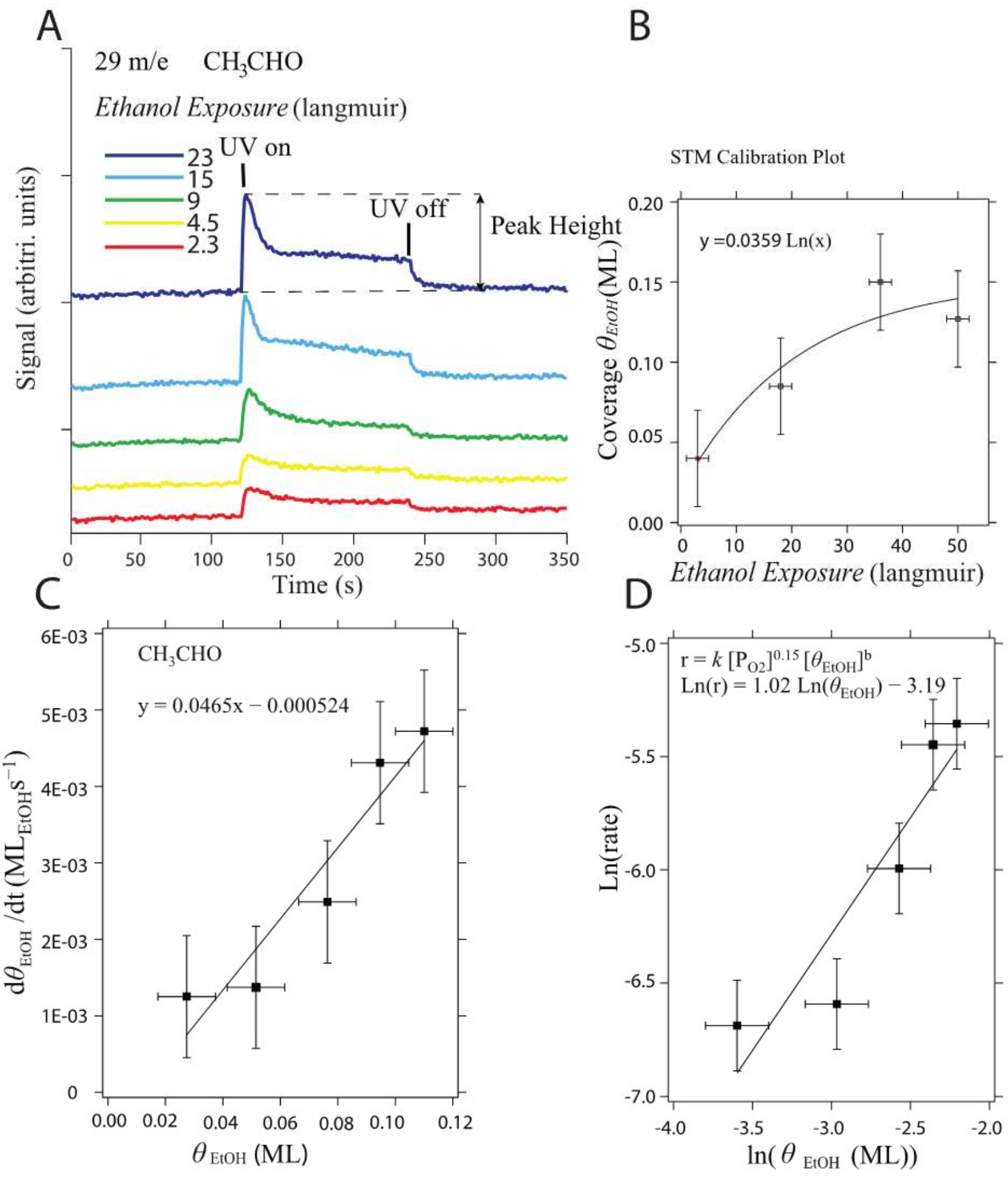

Figure 8.

(**A**) Acetaldehyde formation upon photooxidation of ethanol on TiO_2 (101) at 1×10^{-7} mbar O_2 pressure, 300 K and ethanol exposure between 2.3 and 32 L. (**B**) Ethanol coverage ML plot as a function of exposure in Langmuir. (**C**) Initial rate of reaction ML_{EtOH} s^{-1} with respect to initial ethanol coverage (ML), with a linear regression fit. UV excitation flux = ca. 5mW/cm^2 (D) Ln(rate) vs Ln(θ_{EtOH}) plot.

3.8 Proposed reaction mechanism for the photo-oxidation of ethanol to acetaldehyde over TiO_2(101) anatase single crystal.

The above results suggest the following reaction scheme. Ethanol is first largely dissociatively adsorbed on Ti-O pairs as ethoxides and surface hydroxyls (equation 1) as seen from STM and XPS C 1s results.

$$CH_3CH_2OH(a) + O(s) \rightarrow CH_3CH_2O(a) + OH(a) \qquad \text{(Equation 1)}$$

where (a) stands for adsorbed and (s) for surface.

Upon excitation with UV photons, electrons are excited from the VB of TiO_2 to its CB (equation 2). From the above experimental results, the following reaction steps can be extracted.

$$2\ Ti_s{-}O_s + 2\ h\nu \rightarrow 2\ e^-\ (CB) + 2\ h^+\ (VB) \qquad \text{(also written as } Ti^{3+} \text{ and } O^-(l)\text{)} \qquad \text{(Equation 2)}$$

where (CB) stands for conduction band and (VB) for valence band.

In the presence of O_2, exited electrons lead to O_2^- radical formation (equation 3), which in turn give HOO radicals as previously seen by numerous work[57,58].

$$2\ e^- + 2\ O_2(a) \rightarrow 2\ O_2^-\ (radical) \qquad \text{(Equation 3)}$$

This allows for the first hole trapping by an ethoxide species to give a short-lived oxy-radical species[59] (equation 4).

$$h^+ + CH_3CH_2O(a) + O_s \rightarrow CH_3C^{\bullet}HO(a) + OH(a) \qquad \text{(Equation 4)}$$

An adsorbed molecular ethanol may behave similarly to dissociated ethanol (forming a hydroxy-radical instead of an oxy-radical). Work within our group has demonstrated this favorability in DFT studies[60] of hydrogen peroxide and ethanol[2] with the rutile TiO_2 (110) surface. This is in line with other results of oxygen containing organic adsorbates on TiO_2 surfaces[61].

The formation of the oxy-radical species (equation 4) is followed by a second hole trapping to give acetaldehyde, equation 5.

$$h^+ + CH_3C^{\bullet}HO(a) \rightarrow CH_3CHO(g) \qquad \text{(Equation 5)}$$

The two hydrogen atoms (removed from ethanol (equations 1 and 4)) would ultimately give water to close the cycle, although the initial pathway results in the formation of perhydroxyl radicals (equation 6).

$$2\ O_2^-\ (anion\ radical) + 2\ OH(a) \rightarrow 2\ HOO\ (radical) + 2\ O_s \qquad \text{(Equation 6)}$$

$$2\ HOO\ (radical) \rightarrow 2\ OH\ (radical) + O_2 \qquad \text{(Equation 7)}$$

The sum of equations 1 to 7 gives $CH_2CH_2OH(a) + O_2 \rightarrow CHCHO(g) + 2\ OH\ (radical)$. Oxygen containing radicals would react with a small fraction of the acetaldehyde before desorption to (ultimately) convert it to formate/acetate species. The dependence of the reaction rate with respect to P_{O2} is found to be approximately 0.15, which indicates that other limiting factors (in addition to reaction stoichiometry as seen in the above equations) are involved, in particular the weak equilibrium (binding) constant of O_2 on the surface of TiO_2 which requires increasing pressures for reaction. Oxygen molecules are very weakly adsorbed on TiO_2, in the case of rutile TiO_2 (110) they completely desorb at about 60 K[62], likewise on anatase TiO_2 (101).

The formation of carboxylate species (as hinted by STM in **Figure 5**) and identified by C1s XPS (**Figure 6**) is an evidence of further reactions of the oxy-radical species (as previously seen in photo-oxidation of organic compounds[28,63]). This in turn indicates the participation of oxygen radicals in further reaction steps that ultimately leads to the production of CO_2 and H_2O for a complete catalytic cycle.

4. Conclusions

The photo-catalytic reaction of ethanol over the (101) surface of an anatase TiO_2 single crystal was studied with STM and on-line mass spectrometry in the presence and absence of molecular oxygen. Upon dosing of ethanol at 300 K, two types of species with distinct STM heights are observed. These are attributed to two adsorption modes: molecular and dissociated. UV illumination in the presence of oxygen resulted in the partial depletion of ethanol from the surface. Furthermore, an appearance of large protrusions in the ‘depression’ mode was imaged. These are arranged in a (1×2) structure and oriented along the [010] direction, which strongly suggests that the species are adsorbed in a bi-dentate manner, such as carboxylate species. Upon UV excitation in the presence of O_2, the main reaction product of ethanol photo-oxidation at 300 K was found to be acetaldehyde. The reaction order with respect to O_2 at near saturation coverage of ethanol/ethoxide is found to be approximately 0.15. The

reaction order with respect to ethanol was found to be equal to 1. The photo-oxidation cross section was $1–4\times10^{-19}$ cm^2 from STM and mass spectrometry measurements at ~0.3-1.0×10^{-7} mbar O_2.

Acknowledgements

This work was funded in part by ERC Advanced Grant (GT, ENERGYSURF No. 267768), EU COST Action CM1104, and the Royal Society.

TOC Graphic

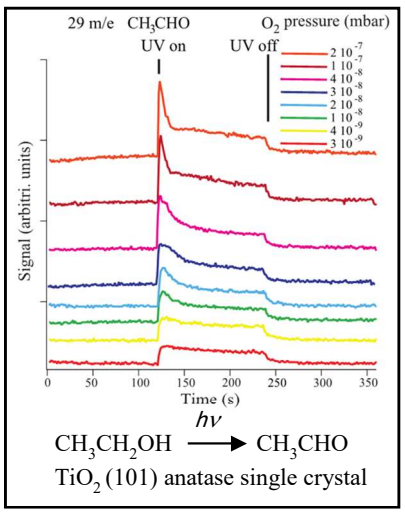
29 m/e CH3CHO
O2 pressure (mbar)
UV on
UV off
2 10-7
1 10-7
4 10-8
3 10-8
2 10-8
1 10-9
4 10-9
3 10-9
Signal (arbitri. units)
0
50
100
150
200
250
300
350
Time (s)
hν
CH3CH2OH
CH3CHO
TiO2 (101) anatase single crystal

5. References

(1) Zehr, R.R.; Henderson, M. A. Acetaldehyde photochemistry on TiO_2(110). *Surf. Sci.* **2008**, *602*, 2238–2249.

(2) Connelly, K. A.; H. Idriss, The photoreaction of TiO_2 and Au/TiO_2 single crystal and powder surfaces with organic adsorbates. Emphasis on hydrogen production from renewables. *Green Chem.* **2012**, *14*, 260-280.

(3) Idriss, H. Barteau, M.A. Active sites on oxides: from single crystals to catalysts. *Adv. in Catalysis* **2000**, *45*, 261- 331.

(4) Henderson, M. A Surface science perspective on TiO_2 photocatalysis. *Surf. Sci. Rep.* **2011**, *66*, 185–297.

(5) Carp, O.; Huisman, C.L.; Reller, A. Photoinduced reactivity of titanium dioxide. *Prog. Solid St. Chem.* **2004**, *32*, 33–177.

(6) Connelly, K.; Wahab, A. K.; Idriss, H. Photoreaction of Au/TiO_2 for hydrogen production from renewables: a review on the synergistic effect between anatase and rutile phases of TiO_2. *Mater. Renew. Sustain. Ener.***2012**, *1*, 1-12.

(7) Tereshchuk, P.; Da Silva, J. Ethanol and Water Adsorption on Close-Packed 3d, 4d, and 5d Transition-Metal Surfaces: A Density Functional Theory Investigation with van der Waals Correction. *J. Phys. Chem. C* **2012**, *116*, 24695-24705.

(8) Wang, Z.; Hao, Q.; Mao, X.; Zhou, C.; Dai, D.; Yang, X. Photocatalytic chemistry of methanol on rutile TiO_2(011)-(2 × 1). *Phys. Chem. Chem. Phys.* **2016**, *18*, 10224–10231.

(9) Pang, C. L.; Lindsay, R.; Thornton, G. Structure of clean and adsorbate-covered single-crystal rutile TiO_2 surfaces. *Chem. Rev.* **2013**, *113)*, 3887-3948.

(10) Al-Azri, Z.; Chen, W. T.; Chan, A.; Jovic, V.; Ina, T.; Idriss, H.; Waterhouse, G. On the role of metals and reaction media in photocatalysis for hydrogen production. Performance evaluation of M/TiO_2 photocatalysts (M = Pd, Pt, Au) for H_2 Production in different alcohol-water mixtures. *J. Catal.* **2015**, *329*, 355-367.

(11) Weststrate, C. J.; Gericke, H. J.; M. W. G. M. Verhoeven, I. M. Ciobîcă, A. M. Saib¶ and J. W. (Hans) Niemantsverdriet; Ethanol Decomposition on Co(0001): C−O bond scission on a close-packed cobalt surface. *J. Phys. Chem. Lett.* **2010**, *1*, 1767-1770.

(12) Alghamdi, H, and Idriss, H. Comparison of the interaction of hydrogen peroxide and ethanol with TiO_2 rutile (110) surface within the context of water splitting. *In preparation*.

(13) Idriss, H.; Seebauer, E. G. Ethanol reactions on oxide surfaces. *J. Mol. Catal. A: Chem.* **2000**, *152*, 201–212.

(14) Guo, Q.; Zhou, C.; Ma, Z.; Ren, Z.; Fan, H. Yang, X.; Elementary photocatalytic chemistry on TiO_2 surfaces. *Chem. Soc. Rev*. **2016**, *45*, 3701–3730.

(15) Thomas, A. G.; Syres, K. L. Adsorption of organic molecules on rutile TiO_2 and anatase TiO_2 single crystal surfaces. *Chem. Soc. Rev*. **2012**, *41*, 4207–4211.

(16) Tan, T. H.; Scott, J.; Ng, Y. H.; Taylor, R. A.; Aguey-Zinsou, K.-F; R. Amal, R. Understanding plasmon and band gap photoexcitation effects on the thermal-catalytic oxidation of ethanol by TiO_2-supported gold. *ACS Catal.* **2016**, *6*, 1870-1879.

(17) Yang, Y. Z.; Chang, C. H.; Idriss, H. Photo-catalytic production of hydrogen from ethanol over M/TiO_2 catalysts (M=Pd, Pt or Rh). *Appl. Catal. B: Environ.* **2006**, *67*, 217-222.

(18) Coronado, J. M.; Kataoka, S.; Tejedor-Tejedor, I. M. A. Anderson The influence of surface properties on the photocatalytic activity of nanostructured TiO_2. *J. Catal.* **2003**, *219*, 219-230.

(19) Yu, Z.; Chuang, S. In situ IR study of adsorbed species and photo-generated electrons during photocatalytic oxidation of ethanol on TiO_2. *J. Catal.* **2007**, *246*, 118-126.

(20) Herman, G. S.; Dohnálek, Z.; Ruzycki, N., Diebold, U. Experimental investigation of the interaction of water and methanol with anatase−TiO_2(101). *J. Phys. Chem. B.* **2003**, *107*, 2788-2795.

(21) Xu, C.; Yang, W.; Guo, Q.; Dai, D.; Chen, M.; Yang, X. Molecular hydrogen formation from photocatalysis of methanol on anatase-TiO_2(101). *J. Am. Chem. Soc*. **2014**, *136*, 602-605.

(22) Xu, M.; Gao, Y.; Moreno, E. M.; Kunst, M.; Muhler, M.; Wang, Y.; Idirss, H.; Wöll, C. Topological features of electronic band structure and photochemistry: new insights from spectroscopic studies on single crystal titania substrates. *Phys. Rev. Lett.* **2011**, *106*, 138302.

(23) Geng, Z.; Chen, X.; Yang, W.; Guo, Q.; Dai, D.; Yang, X. J. Photoinduced carbonyl coupling of aldehydes on anatase TiO_2(101). J. *Phys. Chem. C* **2016**, *120*, 9897−9903.

(24) Zhang, R.; Liu, Z.; Ling, L.; Wang, B. The effect of anatase TiO_2 surface structure on the behavior of ethanol adsorption and its initial dissociation step: A DFT study. *Appl. Surf. Sci.* **2015**, *353*, 150-157.

(25) Thompson, T. L.; Yates, J. T., Jr. Surface science studies of the photoactivation of TiO_2. new photochemical processes. *Chem. Rev*. **2006**, *106*, 4428-4453.

(26) He, Y.; Dulub, O.; Cheng, H.; Selloni, A.; Diebold, U. Evidence for the predominance of subsurface defects on reduced anatase TiO_2 (101). *Phys. Rev. Lett*. **2009**, *102*, 106105-1 to 106105-4.

(27) Kundu, S.; Vidal, A. B.; Nadeem, M. A.; Senanayake, S.D.; Stacchiola, D.; Idriss, H.; Rodriguez, J. A. Ethanol Photoreaction on RuOx/Ru-Modified TiO_2(110). *J. Phys. Chem. C* **2013**, *117*, 11149-11158.

(28) Reztsova, T.; Chang, C. H.; Koresh, J.; Idriss, H. Dark and photoreactions of ethanol and acetaldehyde over TiO_2/Carbon molecular sieve fiber. *J. Catal.* **1999**, *185*, 223–235.

(29) Jayaweera, P. M.; Quah, E. L.; Idriss, H. Photoreaction of ethanol on TiO_2(110) single-crystal surface. *J. Phys. Chem. C* **2007**, *111*, 1764–1769.

(30) Rismanchian, A.; Chen, Y. W.; Chuang, S. In situ infrared study of photoreaction of ethanol on Au and Ag/TiO_2. *Catal. Today* **2016**, *264*, 16-22.

(31) Panayotov, D. A.; DeSario, P. A.; Pietron, J. J.; Brintlinger, T. H.; Szymczak, L. C.; Rolison, D. R.; Morris, J. R. Ultraviolet and visible photochemistry of methanol at 3D mesoporous networks: TiO_2 and Au–TiO_2. *J. Phys. Chem. C* **2013**, *117*, 15035-15049.

(32) King, R.; Idriss, H. Acetone reactions over the surfaces of polycrystalline UO_2. A Kinetic and spectroscopic study. *Langmuir* **2009**, *25*, 4543-4555.

(33) Liao, L. F.; Wu, W. C.; Chen, C. Y.; Lin, J. L. Photooxidation of Formic Acid vs Formate and Ethanol vs Ethoxy on TiO_2 and Effect of Adsorbed Water on the Rates of Formate and Formic Acid Photooxidation. *J. Phys. Chem. B* **2001**, *105*, 7678-7685.

(34) Giannozzi, P.; Baroni, S; Bonini, N.; Calandra, M.; Car, R.; Cavazzoni, C.; Ceresoli, D.; Chiarotti, G. L.; Matteo Cococcioni, M.; *et al.* QUANTUM ESPRESSO: a modular and open-source software project for quantum simulations of materials. *J. Phys. Condens. Matter* **2009**, *21*, 395502.

(35) Garrity, K. F.; Bennett, J. W.; Rabe, K. M.; Vanderbilt, D. Pseudopotentials for high-throughput DFT calculations. *Comp. Mat. Sci.* **2014**, *81*, 446-452.

(36) Murnaghan, F.D. The Compressibility of media under extreme pressures. *PNAS* **1994**, *30*, 1994, 244–247.

(37) Grimme, S. Semiempirical GGA-type density functional constructed with a long-range dispersion correction. *J. Comput. Chem.* **2006**, *27 (15)*, 1787-1799.

(38) Gong, X. Q.; Selloni, A.; Batzill, M.; Diebold, U. Steps on anatase TiO_2(101). *Nat. Mater.* **2006**, *5*, 665-670.

(39) Setvin, M.; Schmid, M.; Diebold, U. Aggregation and electronically induced migration of oxygen vacancies in TiO_2 anatase. *Physical Review B* **2015**, *91*, 195403.

(40) Grinter, D. C.; Nicotra, M.; Thornton, G. Acetic acid adsorption on anatase TiO_2(101). *J. Phys. Chem. C*. **2012**, *116 (21)*, 11643-11651.

(41) Setvin, M.; Daniel, B.; Aschauer, U.; Hou, W.; Li, Y.-F.; Schmid, M.; Selloni, A.; Diebold, U. Identification of adsorbed molecules via STM tip manipulation: CO, H_2O, and O_2 on TiO_2 anatase (101). *Phys. Chem. Chem. Phys.* **2014**, *16*, 21524–21530.

(42) Stetsovych, O.; Todorović, M.; Shimizu, T. K.; Moreno, C.; Ryan, J. M.; León, C. P.; Sagisaka, K.; Palomares, E.; Matolín, V.; Fujita, D.; Ruben, P.; Custance, O. Atomic species identification at the (101) anatase surface by simultaneous scanning tunnelling and atomic force microscopy. *Nat. Commun.* **2015**, *6*, 7265 (1 to 9).

(43) Setvin, M.; Hao, X.; Daniel, B.; Pavelec, J.; Novotny, Z.; Parkinson, G. S.; Schmid, M.; Kresse, G.; Franchini, C.; Diebold, U. Charge trapping at the step edges of TiO_2 anatase (101). *Angew. Chem. Int. Ed.* **2014**, *53*, 4714–4716.

(44) He, Y.; Tilocca, A.; Dulub, O.; Selloni, A.; Diebold, U. Local ordering and electronic signatures of submonolayer water on anatase TiO_2(101). *Nat. Mater.* **2009**, *8*, 585-589.

(45) Hansen, J. Ø.; Huo, P.; Martinez, U.; Lira, E.; Wei, Y. Y.; Streber, R.; Lægsgaard, E.; Hammer, B.; Wendt, S.; Besenbacher, F. Direct Evidence for ethanol dissociation on rutile TiO_2 (110). *Phys. Rev. Lett*. **2011**, *107*, 136102-1 to 136102-4.

(46) Lazzeri, M.; Vittadini, A.; Selloni, A. Structure and energetics of stoichiometric TiO_2 anatase surfaces. *Phys. Rev. B* **2001**, *63*, 155409-1 to 155409-1.

(47) Labat, F.; Baranek, P.; Adamo, C. Structural and electronic properties of selected rutile and anatase TiO_2 surfaces: An ab initio investigation. *J. Chem. Theory Comput*. **2008**, *4*, 341-352.

(48) Nadeem, A. M.; Muir, J.; Connelly, K. A. Ethanol reactions on the surface of rutile TiO_2(110) single crystal. *Physical Chemistry Chemical Physics* **2011**, *13*, 7637-7643.

(49) Quah, E. L.; Wilson, J. N.; Idriss, H. Photoreaction of acetic acid on rutile TiO_2(011) single crystal surface. *Langmuir* **2010**, *26*, 6411-6417.

(50) White, J. M.; Henderson, M. A. Trimethyl Acetate on TiO_2(110): Preparation and anaerobic photolysis. *J. Phys. Chem. B* **2005**, *109*, 12417-12430.

(51) Lu, G.; Linsebigler, A.; Yates, J. T., Jr. The adsorption and photodesorption of oxygen on the TiO_2(110) surface. *J. Chem. Phys.* **1995**, *102*, 4657-4662.

(52) Rohmann, C.; Wang, Y.; Muhler, M.; Metson, J.; Idriss, H.; Wöll, C. Direct monitoring of photo-induced reactions on well-defined metal oxide surfaces using vibrational spectroscopy. *Chem. Phys. Letters* **2008**, *460*, 10-12.

(53) Gao, Y. K.; Traeger, F.; Wöll, C.; Idriss, H. Adsorption, reaction and photo-reaction of the amino acid Glycine on the Surface of ZnO(000ī). *Surf. Sci.* **2014**, *624*, 112-117.

(54) Henderson, M. A. Photooxidation of Acetone on TiO_2(110): Conversion to acetate via methyl radical ejection. *J. Phys. Chem. B* **2005**, *109*, 12062-12070.

(55) Idriss, H.; Légare, P.; Maire, G. Dark and photoreactions of acetates on TiO_2(110) single crystal surface. *Surf. Sci.*, **2002**, *515*, 413-420.

(56) Katsiev, K.; Harrison, G.; Alghamdi, H.; Thornton, G.; Idriss, H. STM and mass spectrometry study of the photo-catalytic oxidation of ethanol to acetaldehyde and formic acid on a rutile TiO_2(110) single crystal. Effect of O_2 partial pressures. *Manuscript in preparation*.

(57) Yang, X.; Tian, P.; Wang, H.; Xu, J.; Han, Y. Catalytic decomposition of H_2O_2 over a Au/carbon catalyst: A dual intermediate model for the generation of hydroxyl radicals. *J. Catal.* **2016**, *336*, 126-132.

(58) Xu, X.; Muller, R.; Goddard, W. The gas phase reaction of singlet dioxygen with water: A water-catalyzed mechanism. *PNAS*, **2002**, *99*, 3376-3381.

(59) Muller, B.; Majoni, S.; Memming, R.; Meissner, D. Particle size and surface chemistry in photoelectrochemical reactions at semiconductor particles. *J. Phys. Chem. B*. **1997**, *101 (14)*, 2501-2507.

(60) Muir, J. N.; Choi, Y.; Idriss, H.; DFT study of ethanol on TiO_2 (110) rutile surface. *Phys. Chem. Chem. Phys.* **2012**, *14*, 11910-11919.

(61) Di Valentin, C.; Fittipaldi, D. Hole scavenging by organic adsorbates on the TiO_2 surface: A DFT model study. *J. Phys. Chem. Lett.* **2013**, *4*, 1901-1906.

(62) Dohnálek, Z.; Kim, J.; Bondarchuk, O.; White, J.M.; Kay, B.D. Physisorption of N_2, O_2, and CO on fully oxidized TiO_2(110). *J. Phys. Chem. B* **2006**, *110*, 6229-6235.

(63) Idriss, H.; Seebauer, E. G. Photooxidation of ethanol on Fe-Ti oxide particulates. *Langmuir* **1998**, *14*, 6146–6150.